Properties and Regulation of a Transiently Assembled ERK2·Ets-1 Signaling Complex†

Kari A. Callaway,[‡,§] Mark A. Rainey,[§,||] Austen F. Riggs,[⊥] Olga Abramczyk,[@] and Kevin N. Dalby*[,‡,||,@,+]

Division of Medicinal Chemistry, Graduate Program in Biochemistry, Graduate Program in Molecular Biology, Center for Molecular and Cellular Toxicology, and Section of Neurobiology, School of Biological Sciences, University of Texas, Austin, Texas 78712-0252

Received May 25, 2006; Revised Manuscript Received September 8, 2006

ABSTRACT: ERK2 is a proline-directed protein kinase that displays a high specificity for a single threonine (Thr-38) on the substrate Ets-1, which lies within the consensus sequence $^{36}\varphi$-χ-Thr-Pro^{39} (where φ is typically a small hydrophobic residue and χ appears to be unrestricted). Thr-38 lies in a long flexible N-terminal tail (residues 1−52), which also contains a second potential phosphorylation site, Ser-26. How Ets-1 binds ERK2 to promote the phosphorylation of Thr-38 while simultaneously discriminating against the phosphorylation of Ser-26 is unclear. To delineate the details of the molecular recognition of Ets-1 by ERK2, the binding of various mutants and truncations of Ets-1 were analyzed by fluorescence anisotropy. The data that were obtained support the notion that the N-terminal tail contains a previously unrecognized docking site that promotes the phosphorylation of Thr-38. This new docking site helps assemble the complex of Ets-1 and ERK2 and makes a similar contribution to the stabilization of the complex as does the pointed domain of Ets-1. The in vitro activation of ERK2 by MKK1 induces a large conformational transition of the activation segment (DFG−APE), but neither induces self-association of ERK2 nor destabilizes the stability of the ERK2·Ets-1 complex. This latter observation suggests that interactions intrinsic to the active site are not important for complex assembly, a notion further supported by the observation that the substitution of a number of different amino acids for Pro-39 does not destabilize the complex. Mutagenesis of ERK2 within loop 13 suggests that Ets-1 binds the substrate-binding groove. These data suggest that ERK2 uses two weak docking interactions to specifically assemble the complex, perhaps in doing so denying Ser-26 access to the active site. Displacement of residues 1−138 of Ets-1 (EtsΔ138) from ERK2 by the peptide N-QKGKPRDLELPLSPSL-C, derived from Elk-1, suggests that Ets-1 engages the D-recruitment site (β7−β8 reverse turn and the αD−αE helix) of ERK2. Displacement of EtsΔ138 from ERK2 by the peptide N-AKLSFQFPS-C derived from Elk-1 shows that EtsΔ138 communicates with the F-recruitment site of ERK2 also.

Extracellular signal-regulated protein kinase 2 (ERK2)[1] has key roles in cellular signal transduction (for reviews, see refs *1*−*8*). It is a ubiquitously expressed, 42 kDa cellular protein kinase that is strongly activated by phorbol esters, growth factors, and serum. The activation of ERK2 often occurs through the action of Ras, a small guanine nucleotide-binding protein that is activated, by a variety of extracellular ligands. Once it is activated, the concentration of ERK2 increases in the nucleus (*9*), where it phosphorylates substrates, many of which are transcription factors. Unregulated activation of ERK2 is associated with tumor growth and progression of metastasis, thereby underlying the need for an understanding of its regulation and cellular specificity.

ERK2 phosphorylates many protein substrates, displaying a strong preference for the consensus sequence φ-χ-Ser/Thr-Pro (*10*−*12*) (where φ is typically a small hydrophobic

† This research was supported in part by the Welch Foundation (F-1390) and the National Institutes of Health (Grant GM59802). K.A.C. was a recipient of a NIH/NIEH predoctoral training grant (ES07247). Mass spectra were acquired by Dr. Herng-Hsiang Lo in the CRED Analytical Instrumentation Facility Core supported by NIEHS Center Grant ES07784. The light scattering measurements were performed at the Light Scattering Facility which has been established with funding from the National Science Foundation (Grant MCB-0237651 to A. F. Riggs). Molecular graphics images were produced using the UCSF Chimera package from the Resource for Biocomputing, Visualization, and Informatics at the University of California, San Francisco (supported by NIH Grant P41 RR-01081).

* To whom correspondence should be addressed: Division of Medicinal Chemistry, College of Pharmacy, University of Texas, Austin, TX 78712. Telephone: (512) 471-9267. Fax: (512) 232-2606. E-mail: Dalby@mail.utexas.edu.

‡ Graduate Program in Biochemistry.

§ Both authors contributed equally to this work.

|| Graduate Program in Molecular Biology.

⊥ Center for Molecular and Cellular Toxicology.

@ Division of Medicinal Chemistry.

+ Section of Neurobiology, School of Biological Sciences.

[1] Abbreviations: 5-IAF, 5′-iodoacetomidofluorescein; BSA, bovine serum albumin fraction V; DTNB, 5,5′-dithiobis(2-nitrobenzoic acid); DTT, dithiothreitol; EDTA, ethylenediaminetetraacetic acid; EGTA, ethylene glycol bis(2-aminoethyl ether)-*N*,*N*,*N*′,*N*′-tetraacetic acid; ERK, extracellular signal-regulated protein kinase; MKK1, MAP kinase kinase 1; ESI, electrospray ionization; EtsΔ138, murine His_6-tagged $Ets1^{1-138}$; EtsΔ138-C31, EtsΔ138 with all cysteine residues except Cys-31 mutated to alanine; EtsΔ138*, EtsΔ138 covalently labeled with fluorescein; HEPES, *N*-(2-hydroxyethyl)piperazine-*N*′-2-ethanesulfonic acid; IPTG, isopropyl β-D-thiogalactopyranoside; MAPK, mitogen-activated protein kinase; K_m^{ets}, Michaelis constant for Ets-1 proteins.

10.1021/bi0610451 CCC: $33.50
Published on Web 11/04/2006

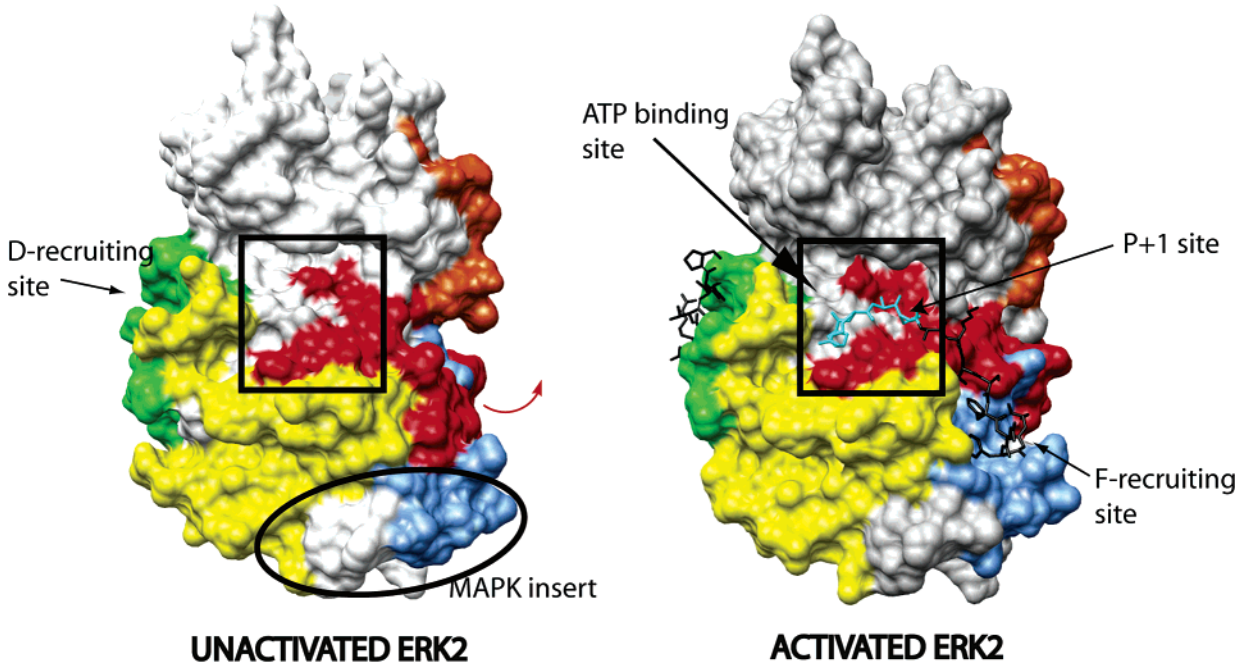

FIGURE 1: Surface representation showing the major conformational changes linking unactivated (*52*) and MKK1-activated ERK2 (*52*). The major conformational change that occurs upon phosphorylation of ERK2 by MKK1 is associated with the activation segment, which is comprised of residues Asp-165−Glu-195 and begins with the DFG motif and ends with the APE motif (colored red). The red arrow indicates the trajectory of the loop upon phosphorylation by MKK1. This segment is phosphorylated on Thr-183 and Tyr-185 by MKK1. Other features are also depicted. The peptide N-*PRSP*AKLSFQFPS-C is shown modeled onto activated ERK2, where *PRSP* is colored cyan (within the box). The substrate-binding groove, comprised of residues in loop 13 (Asn-222−His-230), the αD helix (Leu-110−Thr-116), loop 8 (Gln-117−Ser-120), and the αG helix (Tyr-231−Leu-242), is colored yellow. In addition, several residues in the C-terminus of the MAPK insert (Lys-270−Leu-276) and several residues immediately after this (Phe-277−Asp-281) may also be considered to be part of this groove. The D-recruitment site, comprised of the reverse turn (Asn-156−Asp-160) between the β7 sheet and the β8 sheet, part of loop 7 (Glu-107−Asp-109), the αD helix (Leu-110−Thr-116), loop 8 (Gln-117−Ser-120), and part of the αE helix (Asn-121−Phe-127), and the common docking domain **(**Asp-316 and Asp-319) are colored green.[11] In the F-recruitment site, this pocket shows a preference for phenylalanine at P+6 and P+8, although it should be noted that the specificity has not been rigorously defined. The pocket is comprised of the C-terminus of the activation segment starting at Phe-181 to the end of loop 12 (Phe-181−Thr-204) (as part of the activation loop, this is colored red), the αG helix (Tyr-231−Leu-242), and α2L14 of the MAPK insert helix (Leu-256−Leu-263) (colored blue). In the crystallographic dimerization interface, the proposed dimerization interface is mediated by residues Leu-333, Leu-336, and Leu-344 (colored orange). The MAPK insert (within oval; Ser-246−Leu-276) is implicated in many interactions specific to ERK2.

residue and χ appears to be unrestricted), whose recognition is mediated by interactions that we term as intrinsic to the active site.[2] Most of these interactions are mediated by the sequence known as the activation segment (*13*), which upon phosphorylation by MKK1/2 undergoes a large conformational change (Figure 1, red segment) that is expected to significantly affect the binding sites for the consensus sequence, because the binding pocket for the P+1 Pro is absent in the inactive enzyme (Figure 2). We have been examining the ability of ERK2 to phosphorylate transcription factor Ets-1, a member of the ETS family of transcription factors (*14*−*18*). Recent evidence suggests that the single φ-χ-Thr-Pro motif of Ets-1 does not contribute to the stabilization of the ERK2·EtsΔ138 complex (*18*). This is interesting as this sequence represents the only motif that is recognized by the active site of the enzyme, and therefore, understanding how the consensus sequence of a protein is selected by ERK2 remains an important question to answer.

Members of the protein kinase family frequently utilize a region of the catalytic domain called the extended substrate-binding groove, to recognize protein substrates (*19*). In ERK2, this conserved region is comprised of residues in loop 13, the αD helix, loop 8, and the αG helix. In addition, several residues in the C-terminus of the MAPK insert, as well as some residues immediately after this, may also contribute to this site (Figure 1). ERK2 employs recruiting sites that are thought to bind discrete substrate motifs termed docking sites (*20*). Two relatively common MAPK-docking sites have been identified in proteins.[3] The F-site is reported to have a Phe-χ-Phe-Pro consensus sequence (*9*) and has been found primarily in ERK2 substrates (*21*−*23*). This site is usually found C-terminal to a φ-χ-Ser/Thr-Pro motif and binds a hydrophobic pocket of ERK2 that is formed by the C-terminus of the activation segment, the αG helix, and the α2L14 helix of the MAPK insert (see Figure 1, activated, which shows the *PRSP*AKLSFQFPS peptide modeled on the surface of activated ERK2) (*24*). Note how the activation segment of unactivated ERK2 occludes this pocket (Figure 1, unactivated). The D-site is best described as a cluster of basic amino acids located N-terminal to a hydrophobic ϕ-X-ϕ motif (ϕ is often Leu, Ile, or Val) (*21*). The D-site has been found in substrates of ERK2 as well as in substrates of JNK

[2] We define those interactions that bind residues φ-χ-Ser/Thr-Pro (P−2 to P+1) of the protein substrate as being intrinsic to the active site.

[3] Two docking sites termed D-sites and F-sites have been identified on MAPK ligands. The sites on MAPKs that recognize D-sites or F-sites are termed D-recruitment or F-recruitment sites, respectively. D-Sites have also being called DEJL domains, while F-sites have also being called DEF domains or Phe-X-Phe domains.

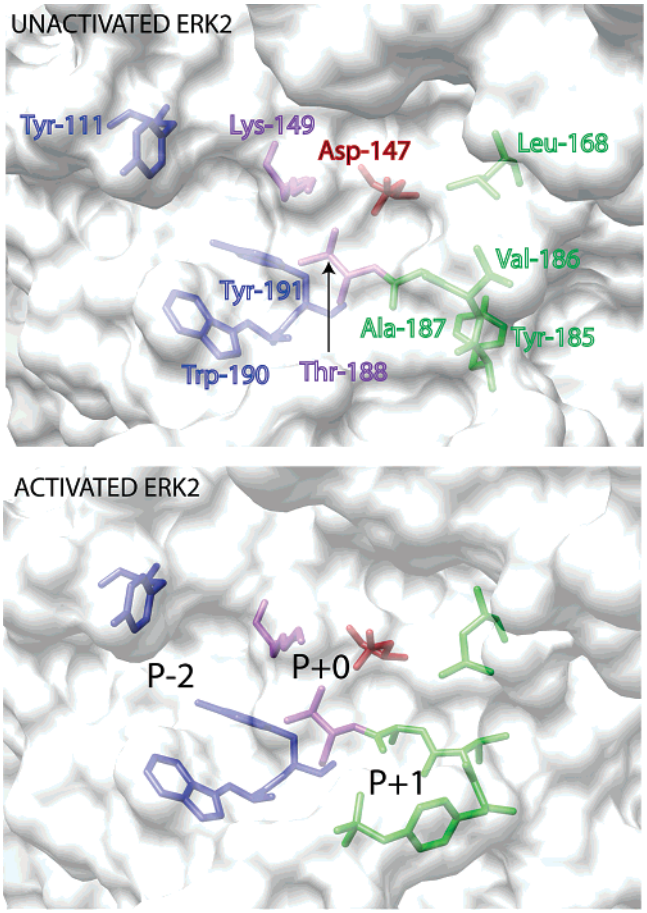

FIGURE 2: Effect of activation on the conformations of the consensus sequence, $^{36}\varphi$-χ-Thr-Pro^{39}, binding pocket. The P−2 binding pocket is based on a structural alignment with CDK2 (PDB entry 1QMZ) (*62*); the putative hydrophobic pocket for P−2 residues is comprised of Tyr-111, Lys-149, Thr-188, Trp-190, and Tyr-191. The P0 binding site pocket is comprised of Asp-147, Lys-149, and Thr-188. The P+1 binding pocket is comprised of the side chains of Leu-168 and pTyr-185 and the backbone of pTyr-185−Ala-187 (see the boxes in Figure 1).

and p38 MAPKα (*25*−*27*). The D-sites are typically found N-terminal to φ-χ-Ser/Thr-Pro motifs, often, more than 30 amino acids away and bind the D-recruitment site, which is a groove comprised of the reverse turn between the β7 and β8 sheets, part of loop 7, the αD helix, loop 8, and part of the αE helix (Figure 1). Interestingly, unlike the F-recruitment site, this pocket is largely unaffected by the activation state of ERK2.

Members of the ETS family contain a conserved 85-amino acid domain that binds to the DNA sequence 5′-GGA(A/T)-3′ (*28*). Despite binding to similar DNA sequences, ETS proteins regulate quite diverse processes (*29*). Ets-1 binds at *ras* response elements, in response to Ras signaling, which triggers the phosphorylation of Ets-1 by ERK2 (*30*). A feature present in Ets-1 and conserved in ∼40% of the *ets* gene family members is the pointed domain (PNT domain). The PNT domain contains an ERK2 docking site that has been located to a span of residues ^{114}Leu−Phe^{120}, a site that appears to be unique to this domain (Figure 3) (*31*). Our work has shown that ERK2−Ets-1 interactions, governing the phosphorylation of Thr-38 by ERK2, are transient in nature with lifetimes of just a few milliseconds (*15*) and that ERK2 catalyzes the phosphorylation of Thr-38 with remarkable specificity (*15*), so high in fact that no Ser-26 phosphorylation is detected, even after extensive incubation. This is impressive, because amino acids 1−52 are highly flexible in EtsΔ138 and Ser-26 is just 12 amino acids N-terminal to the site of phosphorylation (Figure 3, note residues 1−29 are not shown). However, it should be noted that the phenylalanine in the P−2 position (Figure 3B) is thought to slightly disfavor the phosphorylation of substrates by ERK2 (*10*).

Major questions concern the structure and stability of ERK2 signaling complexes and how these features relate to both their regulation and ERK2's catalytic mechanism. In the course of our work (*15*−*18*, *32*), we have provided quantitative thermodynamic information and kinetic information, which we anticipate will help attempts to model MAPK signaling systems in silico (*33*−*40*). Here we have focused on the mechanism of recognition of Ets-1 by ERK2. Considerations of the mechanism of phosphorylation of Ets-1 by ERK2 led us to consider two possible roles for the docking site in the pointed (PNT) domain of Ets-1. We considered the possibility that it orients the flexible N-terminus to take advantage of the preferred conformations of the N-terminus, while as an alternative proposal, we considered the possibility that it promotes the binding of the N-terminus to a site within the complex. To test these models, we analyzed the binding of ERK2 to truncations and mutants of Ets-1. The data that were obtained support the notion that the N-terminal tail contains a previously unrecognized docking site that promotes the phosphorylation of Thr-38. Displacement of Ets-1 from ERK2 by peptides derived from the D-site and F-site of Elk-1 suggests that Ets-1 communicates with both known recruitment sites. Finally, light scattering analysis of several solutions of activated ERK2 suggests that while ERK2 may have a propensity to self-associate it does not appear to be an obligate result of activation.

EXPERIMENTAL PROCEDURES

Reagents. Ultrapure grade Tris was obtained from ICN Biomedicals (Aurora, OH). 5′-Iodoacetamidofluorescein (5-IAF) was purchased from Molecular Probes (Eugene, OR). 5,5′-Dithiobis(2-nitrobenzoic acid) and all other chemicals were from Sigma (St. Louis, MO). *Escherichia coli* strain DH5α, used for cloning and isolation of plasmids, was obtained from Invitrogen. *E. coli* strain BL21(DE3), used for recombinant protein expression, was purchased from Novagen (Madison, WI). Tryptone, yeast extract, and agar were obtained from US Biologicals (Swampscott, MA) and BD (Sparks, MD), respectively. The Mono-Q HR 10/10 anion exchange column and PD-10 desalting columns were purchased from Amersham Biosciences (Piscataway, NJ). Qiagen Inc (Valencia, CA) supplied the Ni−NTA agarose and the Qiaprep Spin miniprep kit. Ambion, Inc. (Austin, TX), provided the thin-walled PCR tubes. Restriction enzymes, PCR reagents, and T4 DNA ligase were from Hoffmann-La Roche, Ltd. (Basel Switzerland), Promega Corp. (Madison, WI), or New England Biolabs (Beverly, MA). Oligonucleotides for DNA amplification and sequencing were from Genosys (The Woodlands, TX). The remaining molecular biology reagents, including DNA ladders and protein molecular mass standards, were obtained from Invitrogen Corp. (Carlsbad, CA).

General Methods. Techniques for restriction enzyme digestion, ligation, transformation, and other standard mo-

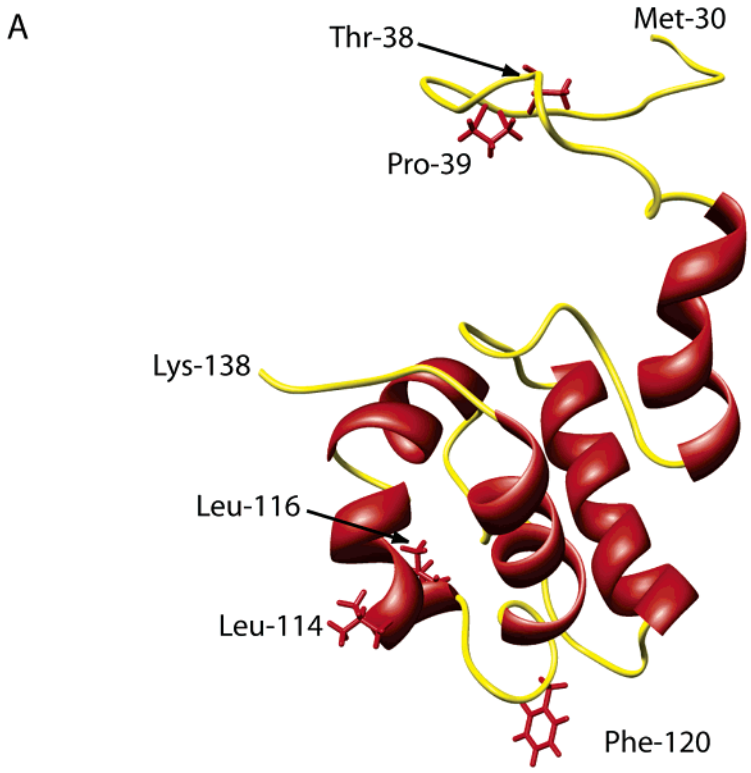

B

```
Ets-2   1    MNDFGIKNMDQVAPVANSFRGTLKRQPAFDTFDGSLFAVLPSLSEDQTLQEVPTGLDSVS  60
Ets-1   1    ------------------MKAAVDLKPTLTIIK----------TEKVDLELFP------S  26

Ets-2   61   HDSASCELPLLTPCSKAVMSQALKATFSGFQKEQRRLGIPKNPWLWSEQQVCQWLLWATN  120
Ets-1   27   PDMECADVPLLTPSSKEMMSQALKATFSGFTKEQQRLGIPKDPRQWTETHVRDWVMWAVN  86

Ets-2   121  EFSLVNVNLHQFGMNGQMLCNLGKERFLELAPDFVGDILWEHLEQMIKENQEKTEDQYEE  180
Ets-1   87   EFSLKGVDFQKFCMSGAALCALGKECFLELAPDFVGDILWEHLEILQKED----------  136
```

FIGURE 3: (A) Structure of EtsΔ138. Ribbon diagram of EtsΔ30−138 (PDB entry 1BQV) (*63*) showing residues Leu-114, Leu-116, and Phe-120 that are important for ERK2 binding. Note this is just one conformation determined by NMR (*63*). (B) Sequence alignment of mouse Ets-1 (residues 1−136) with the corresponding sequence of mouse Ets-2 (residues 1−180) using CLUSTAL W (1.83). Residues Leu-114, Leu-116, and Phe-120 (Ets-1 numbering) in the PNT domain, known to be involved in ERK2 docking, are colored red. Residues in the PNT domain are colored blue. Residues in the flexible N-terminal tail are colored black. Identical residues share a pink background; similar hydrophobic residues share a green background, and similar charged residues share a red or blue background. The GenBank accession numbers for the Ets-1 and Ets-2 sequences are CAA37904 and AAA37581, respectively.

lecular biology manipulations were based on methods described by the manufacturer. Plasmids were introduced into cells using a BTX Transporter Plus device. UV−vis absorbance readings were taken on a Varian Cary Model 50 spectrophotometer. FPLC was performed on a Pharmacia ÄKTA FPLC system. HPLC was conducted on a Waters HPLC system using a 250 mm × 4 mm Vydac RP C18 column (#218TP54). Protein was analyzed by Tris-glycine sodium dodecyl sulfate−polyacrylamide gel electrophoresis (SDS−PAGE) under denaturing conditions on 10 to 15% gels using the Bio-Rad Mini-protean III vertical gel electrophoresis apparatus.

Peptides. Peptides, synthesized at the University of Texas Molecular Biology core facilities, were raised in water and brought to pH 7.5 by the addition of sodium hydroxide. The concentration of each peptide was determined by amino acid analysis. The following peptides were used: Elk-1 F-site [N-AKLSFQFPS-C (1024 Da) (*21*)] and Elk-1 D-site [N-QKGKPRDLELPLSPSL-C (1934 Da) (*25*)]. The molecular mass of each peptide was determined by MALDI mass spectrometry.

Expression and Purification of Proteins. Methods for the expression of ERK2 and MKK1G7B and the method of ERK2 activation are included in the Supporting Information. Further details are reported elsewhere (*15*, *17*).

His_6-Tagged EtsΔ138-C31 and EtsΔ138-C99. The EtsΔ138-C31 and EtsΔ138-C99 constructs generated from site-directed mutagenesis were used to express the mutant as an N-terminal hexahistidine fusion protein. The pET-28a plasmid containing the DNA for the desired Ets-1 cysteine mutant was transformed by electroporation at 1.8 V into *E. coli* BL21(DE3) cells. Cells were grown at 30 °C in Luria broth containing 20 μg/mL kanamycin to an optical density of 0.8 before being induced with 0.5 mM IPTG. The cells were cultured for an additional 5 h at 30 °C before being harvested. Cells were lysed in 150 mL of lysis buffer [20 mM Tris (pH 8.0), 0.5 M NaCl, 5 mM imidazole, 0.03% (by mass) Brij-30, 0.1% (v/v) β-mercaptoethanol, 1% (by mass) Triton X-100, 1 mM benzamidine, 0.1 mM PMSF, and 0.1 mM TPCK]. The suspension was sonicated for 20 min (5 s pulses with 5 s intervals) at 4 °C. The lysate was cleared (16 000 rpm for 25 min at 4 °C) and the supernatant

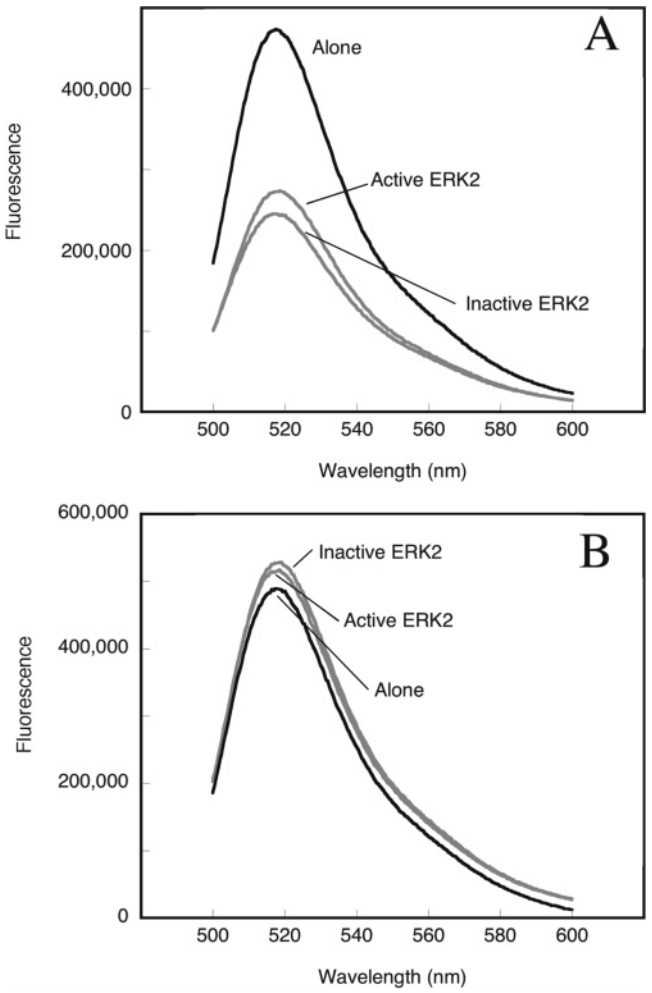

FIGURE 4: Characterization of the fluorescent properties of EtsΔ138-C31* and EtsΔ138-C99*. The fluorescence emission spectrum of 100 nM EtsΔ138-C31* (A) or 100 nM EtsΔ138-C99* (B) was examined in the absence (black) and presence (gray) of 20 μM active and inactive ERK2. The sample was excited with light at 492 nm, and an emission scan was performed from 500 to 600 nm.

agitated gently with 20 mL of Ni−NTA beads (Qiagen). The beads were washed with 150 mL of wash buffer [20 mM Tris (pH 8.0), 0.03% (by mass) Brij-30, 0.1% (v/v) β-mercaptoethanol, 1 mM benzamidine, 0.1 mM PMSF, 0.1 mM TPCK, and 10 mM imidazole], and His_6-EtsΔ138-C31 or His_6-EtsΔ138-C99 was eluted with 100 mL of elution buffer [20 mM Tris (pH 8.0), 0.03% (by mass) Brij-30, 0.1% (v/v) β-mercaptoethanol, 1 mM benzamidine, 0.1 mM PMSF, 0.1 mM TPCK, and 200 mM imidazole]. The eluted protein was loaded onto a MonoQ HR 10/10 anion exchange column that had been pre-equilibrated in anion exchange buffer [20 mM Tris (pH 8.0), 0.03% (by mass) Brij-30, and 0.1% (v/v) β-mercaptoethanol]. The column was developed with a gradient of 0 to 250 mM NaCl over 17 column volumes, and the protein was eluted at 59−105 mM NaCl. Collected fractions were combined and dialyzed into dialysis buffer [25 mM HEPES (pH 7.5), 50 mM KCl, 0.1 mM EDTA, 0.1 mM EGTA, and 2 mM DTT]. The concentrations of EtsΔ138-C31 and EtsΔ138-C99 were established using an extinction coefficient (A_{280}) of 22 880 cm^{-1} M^{-1}.

Each EtsΔ138 construct and mutant was generated and purified essentially as described previously (*14*) and dialyzed into 1.25 mM Hepes (pH 7.5), 2.5 mM KCl, and 2 mM DTT. All proteins produced from the pET-28a vector have an N-terminal sequence of Met-Gly-Ser-Ser-His-His-His-His-His-His-Ser-Ser-Gly-Leu-Val-Pro-Arg-Gly-Ser-His prior to the initial methionine encoded by the EtsΔ138 cDNA; however, usually, the initial methionine is cleaved after production in bacteria (*14*). All EtsΔ138 constructs used here have a Ser26Ala mutation (*17*).[4]

Removal of the His Tag. To test whether the His_6 tag used to purify EtsΔ138 affects the affinity of the ERK2·EtsΔ138-F docking complex, we cleaved it from EtsΔ138 using thrombin to give ΔHisEtsΔ138. ΔHisEtsΔ138 was purified by MonoQ HR 10/10 anion exchange chromatography (eluted at 0.17 M NaCl). Cleavage was confirmed by SDS−PAGE and mass spectrometry following reverse phase chromatography on a C-18 column (observed mass of 15 912 Da; expected mass of 15 914 Da) (see the Supporting Information). A competition analysis (data not shown) revealed that ΔHisEtsΔ138 binds ERK2 with a 1.5-fold decrease in affinity compared to that of EtsΔ138.

Labeling of EtsΔ138-C31 and EtsΔ138-C99 with Fluorescein. 5′-Iodoacetamidofluorescein (5-IAF) was used to covalently attach a fluorescein moiety to the single cysteine residue present in EtsΔ138-C31 and EtsΔ138-C99. Prior to the reaction with 5-IAF, the protein was dialyzed overnight at 4 °C into 2 L of labeling buffer [20 mM HEPES (pH 7.3), 50 mM KCl, and 2 mM EDTA] to remove DTT. A fresh stock of 10 mM 5-IAF was made in dimethylformamide (DMF) and kept in the dark. The stock concentration was determined by measuring the absorbance at 492 nm (ϵ_{492} = 78 000 cm^{-1} M^{-1}). Since the absorption of fluorescein is pH sensitive, the absorbance readings were taken in 20 mM HEPES (pH 7.5). To initiate the labeling reaction, 5-IAF (10:1 molar ratio) was added dropwise to a solution of the protein in labeling buffer. The reaction was allowed to proceed overnight at 4 °C in the dark. After 13−14 h, the reaction was quenched by addition of a 10-fold molar excess of β-mercaptoethanol. The sample was then concentrated to a volume of 2.5 mL and applied to a PD-10 desalting column (Amersham) to remove any unreacted 5-IAF. The labeled protein was further purified by anion exchange chromatography using a MonoQ HR 10/10 column. A gradient from 0 to 250 mM NaCl was applied over 17 column volumes, and the fluorescein-labeled protein eluted at 219 mM NaCl. The collected fractions were dialyzed overnight at 4 °C in dialysis buffer [25 mM HEPES (pH 7.5), 50 mM KCl, 0.1 mM EDTA, 0.1 mM EGTA, and 2 mM DTT]. Labeling of the protein was verified by ESI mass spectrometry following elution from a reverse phase C1 Vydac (218TP54, 25 cm × 4 mm) column (0 to 100% acetonitrile, 80 min, 0.6 mL/min) (see the Supporting Information for further details).

Tryptic Digest of EtsΔ138-C31.* To confirm the site of fluorescein labeling, a tryptic digest was carried out on EtsΔ138-C31*. Approximately 2 mg of protein was dialyzed overnight at 4 °C in 25 mM ammonium carbonate (pH 8.6). The protein was then digested overnight at 37 °C with 25 μg of trypsin (Promega). The entire digest was then injected onto a C18 reverse phase C1 Vydac (218TP54, 25 cm × 4 mm) column that had been pre-equilibrated in 0.1% (v/v) TFA. The column was developed with a linear gradient

[4] Pro-39Ala contains Ser-26.

from 0 to 100% acetonitrile [containing 0.1% TFA (v/v)] over 90 min at a rate of 0.6 mL/min. The fluorescein-labeled peptide eluted at 56% acetonitrile. Electrospray ionization mass spectrometry identified V^{19}DLELFPAPDMEC^{31}-ADVPLLTPSSK^{42} as the peptide modified by covalent addition of a fluorescein moiety.

Examining the Fluorescence Properties of Fluorescein-Labeled Proteins. To investigate the spectral properties of EtsΔ138-C31* and EtsΔ138-C99*, 100 nM protein was examined in 25 mM HEPES (pH 7.5), 50 mM KCl, 40 μg/mL BSA, 0.1 mM EDTA, 0.1 mM EGTA, 1.3% glycerol, and 2 mM DTT in a final volume of 60 μL. Fluorescence measurements were taken at 27 °C using a Fluorolog model FL3-11 fluorometer (Jobin Yvon, Edison, NJ) using three-window fluorescence grade quartz cuvettes with a path length of 1.0 cm and an aqueous volume of 55 μL purchased from Helma (Plainview, NY). To determine the excitation maximum, an excitation scan was performed from 450 to 500 nm. Slit widths were set to 2.5 nm; the integration time for each reading was 500 ms, and the emission was monitored at 517 nm. For determination of the emission maximum, fluorescein-labeled proteins were excited with light at 492 nm and an emission scan was performed from 500 to 600 nm. Slit widths were set to 2.5 nm, and the integration time for each reading was 500 ms.

To determine the effect of binding on the fluorescence yield, the fluorescence emission was examined in the absence and presence of 20 μM ERK2. Assays were performed in 25 mM HEPES (pH 7.5), 50 mM KCl, 40 μg/mL BSA, 0.1 mM EDTA, 0.1 mM EGTA, 1.3% glycerol, and 2 mM DTT containing 100 nM EtsΔ138-C31* or EtsΔ138-C99* in a final volume of 60 μL. The protein was excited with polarized light at 492 nm, and an emission scan was performed from 500 to 600 nm. Slit widths were set to 2.5 nm, and the integration time for each reading was 500 ms. The resulting peaks on the emission scans were then integrated to determine the ratio of the fluorescence yield of the bound fluorophore to the free fluorophore, *R*. *R* was also calculated from the anisotropy experiments by measuring the polarized intensities for the free and bound form of the fluorophore, according to eq 1

$$R = \frac{(I_V + 2GI_H)_{bound}}{(I_V + 2GI_H)_{free}} \quad (1)$$

where I_V and I_H are the intensity of the emission at polarizations both parallel and perpendicular to the excitation source, respectively, and *G* is a factor that corrects for instrumental differences in the detection of emission components. Specifically, the *G* factor is the ratio of the intensity of the vertically and horizontally polarized emission components when the sample is excited with horizontally polarized light.

Fluorescence Anisotropy Binding Assays. Assays were performed under the conditions described above. Instrument Control Center (Jobin Yvon) was used to collect data and to calculate the fluorescence anisotropy, *r*, which is defined as

$$r = \frac{I_V - GI_H}{I_V + 2GI_H}$$

The protein was excited with polarized light at 492 nm, and the horizontal and vertical components of the emitted light were detected at 515 nm. Excitation and emission slit widths were set to 2.5 nm, and the integration time for each reading was 300 ms. Measurements were taken every 15 s for a total of 3 min, and the resulting anisotropy values were averaged. The dissociation constants were determined by fitting the average anisotropy values to eq 2 (defined in the Supporting Information) using Kaleidgraph 4.0 (Synergy Software). Where r_f and r_b are the anisotropies of the free and bound fluorescein-labeled protein, respectively, *R* is the ratio of fluorescent yields of the bound form and the free form, $[S_t]$ and $[E_t]$ are the total concentrations of the fluorescein-labeled protein and ERK2, respectively, and K_d is the dissociation constant.

Fluorescence Anisotropy Competition Experiments. Assays were performed in 25 mM HEPES (pH 7.5), 50 mM KCl, 40 μg/mL BSA, 0.1 mM EDTA, 0.1 mM EGTA, 1.3% glycerol, and 2 mM DTT containing 10 μM ERK2, 100 nM EtsΔ138-C31*, and varied concentrations of the competing protein in a final volume of 60 μL. Each reaction mixture was equilibrated to 27 °C before being excited with vertically and horizontally polarized light at 492 nm. Emission at both the vertical and horizontal positions at 515 nm was measured every 15 s for 3 min. Excitation and emission slit widths were set to 2.5 nm, and the integration time for each reading was 300 ms. The average anisotropy values were calculated and fit using eqs 3−7 in Scientist (Micromath)

$$r = (\{[K_d + [S_t] + [E_t] - \sqrt{(-K_d - [S_t] - [E_t])^2 - 4[E_t][S_t]}]/(2[S_t])\} \times (r_bR - r_f) + r_f)/(1 + \{[K_d + [S_t] + [E_t] - \sqrt{(-K_d - [S_t] - [E_t])^2 - 4[E_t][S_t]}]/(2[S_t])\}(R - 1)) \quad (2)$$

$$r = \frac{\frac{[ES]}{[S_t]}(r_bR - r_f) + r_f}{1 + \frac{[ES]}{[S_t]}(R - 1)} \quad (3)$$

$$[E\cdot S] = \frac{[E_f][S_t]}{K_d + [E_f]} \quad (4)$$

$$K'_d = \frac{[E_f][B_f]}{[E\cdot B]} \quad (5)$$

$$B_t = B_f + [E\cdot B] \quad (6)$$

$$E_t = E_f + [E\cdot B] + [E\cdot S] \quad (7)$$

where S, B, and E correspond to the fluorescein-labeled EtsΔ138-C31*, an unlabeled competitor, and ERK2, respectively. The subscript f and b correspond to free and bound forms, respectively. K' < rmark>$_d$ corresponds to the dissociation constant for the E·B complex.

Scheme 1: Schematic Representation of Ets-1 Constructs[a]

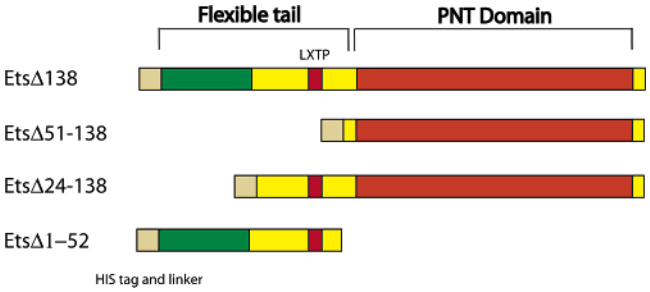

[a] The red square corresponds to the consensus motif recognized by the active site of ERK2.

Light Scattering Experiments. Prior to light scattering experiments, ERK2 was dialyzed into 25 mM HEPES (pH 7.5), 50 mM KCl, 2 mM DTT, 0.1 mM EDTA, and 0.1 mM EDTA. Multiangle laser light scattering experiments were performed on three separate concentrations of active ERK2 (16, 32, and 48 μM). A Dawn model EOS multiangle light scattering photometer (Wyatt Technology, Santa Barbara, CA) with a 30 mW GaAs linearly polarized laser with a wavelength of 685 nm was used in all experiments. The photometer has a K5 flow cell maintained at 25 °C and has a volume of 67 μL and a scattering volume of ~0.5 μL. High-gain photodiodes are placed at 18 scattering angles. A Shimadzu LC-10 ADvp HPLC pump with a Rheodyne model 7725 injection valve outfitted with a 20 μL sample loop was used to deliver samples through a Bio-Gel 40XL column (300 mm × 7.8 mm, Bio-Rad catalog no. 125-0604), now available as a TSK-GEL G4000PWXL column [7.8 mm (inside diameter) × 30 cm, catalog no. 08022, Tosoh Bioscience, Montgomeryville, PA] followed in series by a TSK-GEL G3000PWXL column [300 mm × 7.8 mm (inside diameter), catalog no. 08021]. The total column volume is ~15 mL. The buffer [25 mM HEPES (pH 7.5), 50 mM KCl, 2 mM DTT, 0.1 mM EDTA, and 0.1 mM EDTA], freshly prepared with nanopure water (~18.3 MΩ cm) and filtered through a 0.02 μm filter (Anodisc 47, Whatman, catalog no. 6809-5002), was used to establish the light scattering baseline. Size exclusion chromatography was carried out at a flow rate of 0.5 mL/min at room temperature with a run time of ~60 min. Samples were centrifuged for ~30 s to remove any insoluble components prior to injection. No filtration devices were used.

RESULTS

Examining the Importance of ERK2 Phosphorylation

Preparation and Characterization of Fluorescent EtsΔ138. To investigate the mechanism by which ERK2 and Ets-1 recognize each another, we developed a fluorescence binding assay using single-cysteine mutants of Ets-1, which were specifically labeled with a fluorophore. A truncated version of Ets-1 was used in this assay termed EtsΔ138 (see Scheme 1 and Figure 3). This protein is phosphorylated at Thr-38 with steady-state parameters (k_{cat} and K_m^{ets}) identical to those of full-length Ets-1, suggesting that all the important contacts within the E•S complex are mediated by the 138 N-terminal residues of Ets-1 (*31*). Relative to ERK2, which is 42 kDa, EtsΔ138 is a small 17 kDa protein, and therefore, when labeled with a suitable flurophore, it is predicted to furnish

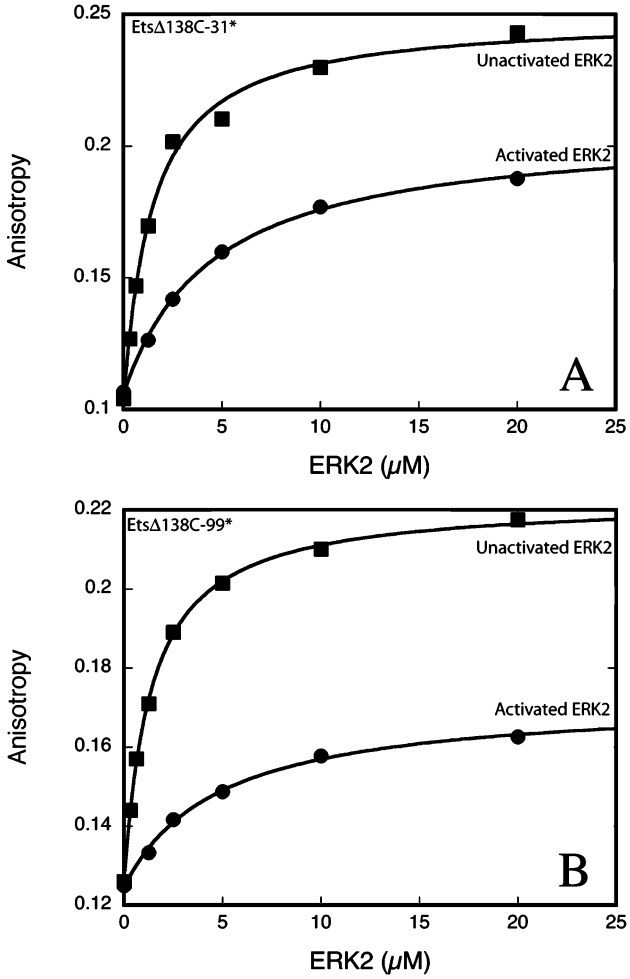

FIGURE 5: Binding of EtsΔ138-C31* and EtsΔ138-C99* to active and inactive ERK2. (A) Binding of 100 nM EtsΔ138-C31* to active (●) and inactive (■) ERK2 (0−20 μM). (B) Binding of 100 nM EtsΔ138-C99* to active (●) and inactive (■) ERK2 (0−20 μM). Anisotropy values were averaged, and the dissociation constants were determined by fitting the average anisotropy values to eq 2 using Kaleidgraph 4.0 (Synergy Software). *R* values of 0.5 (EtsΔ138-C31*) and 1.0 (EtsΔ138-C99*) were used in eq 2.

an observable change in fluorescence anisotropy upon binding ERK2. As EtsΔ138 contains four cysteines, these were mutated to provide two single-cysteine derivatives. These were generated, purified, and then labeled with fluorescein, as described in Experimental Procedures and the Supporting Information, to give two singly labeled proteins, EtsΔ138-C31* or EtsΔ138-C99*. Panels A and B of Figure 4 show that both proteins exhibit excitation and emission λ_{max} similar to those of fluorescein and that the fluorescence yield of EtsΔ138-C31*, but not EtsΔ138-C99*, decreases 2-fold upon ERK2 binding.[5]

EtsΔ138 Forms a Weak Complex with both Activated and Unactivated ERK2. To examine the binding of EtsΔ138-C31* to MKK1-activated ERK2, a 100 nM solution (final concentration) of EtsΔ138-C31* was added to varying concentrations of activated ERK2 and the resulting anisotropy determined [Figure 5A (●)]. As expected, the anisotropy values increased upon addition of ERK2, consistent with the

[5] Notably, a change in fluorescence intensity may be used to follow the binding of ERK2, and in other studies, we have used this to examine binding under stopped-flow conditions.

formation of an EtsΔ138-C31*·ERK2 complex. Similar results were seen for EtsΔ138-C99* [Figure 5B (●)].

Activated ERK2 forms crystallographic homodimers that display a 2-fold axis of symmetry with both active sites on the same face of the complex that is reported to persist in solution and play a role in both ERK2 regulation and possibly also substrate recognition (*41*). To see whether the activation state of ERK2 was important for substrate binding, the anisotropy experiment was repeated with unactivated ERK2. Remarkably, the anisotropy values increased in a manner similar to that of the first experiment, where activated ERK2 was used [Figure 5A (■)], indicating that EtsΔ138 assembles on the surface of both forms of ERK2 with a similar affinity. Thus, the activation state of ERK2 does not appear to regulate its ability to bind Ets-1. Interestingly, the observed change in anisotropy, upon the addition of unactivated ERK2, was always greater than the change observed upon addition of activated ERK2 (Figure 5A,B). A greater anisotropy value for a complex is consistent with a slower rotating complex, which is the result of either greater size or different shape.

Assessing the Role of ERK2 Self-Association

Recognition of Ets-1 Is Mediated by the ERK2 Monomer. As the anisotropy of the inactive ERK2·EtsΔ138-C99 complex was higher than that of the active complex at all concentrations of added ERK2 (Figure 5A,B), we decided to test whether activated ERK2 has a propensity to self-associate under the conditions of our experiment. To examine the ability of activated ERK2 to self-associate, we subjected three different concentrations (16, 32, and 48 μM) of activated ERK2 to gel filtration through a Bio-Gel 40XL column linked in series to a TSK-GEL G3000PWXL column, and then multiangle laser light scattering experiments were performed on the eluted fractions. The molar mass distribution, as a function of elution volume, is shown for each sample in Figure 6A. This figure shows that the protein that elutes at 17−28 mL displays little deviation from a mass of ~41 kDa, and in fact, the data for the three concentrations can be virtually superimposed on each other. The concentrations of the central major peaks (determined at the peak maximum) were ~58 μg/mL (1.4 μM), 132 μg/mL (2.9 μM), and 197 μg/mL (3.4 μM), and the calculated masses for these three concentrations did not differ significantly from 41 188 ± 330 Da. Analysis of the cumulative molar mass distribution is shown in Figure 6B. This figure, encompassing all the data between elution volumes of 14−28 mL, shows that masses greater than ~41−42 kDa cannot comprise more than ~1% of the total protein.[6] Estimates of very small contributions to the total cannot be very accurate, because they depend critically on the precise position of the baseline and are subject to substantial noise. Between 16 and 17 mL, the apparent masses are 45−55 kDa, and at ~14 mL, the apparent mass is in the range of ~90−100 kDa. However, although the apparent masses of the molecules eluting between 14 and 18 mL suggest some association, the quantities involved are vanishingly small and could be produced by a minor error in the apparent baseline. Overall, these experiments demonstrate that activated ERK2 shows no propensity to self-associate and support the notion that the major complexes in the binding assays are heterodimers of ERK2 and EtsΔ138.

[6] The dip in the apparent mass near 19 mL is of uncertain origin but could be due to a contaminant with a lower mass or the result of proteolytic degradation.

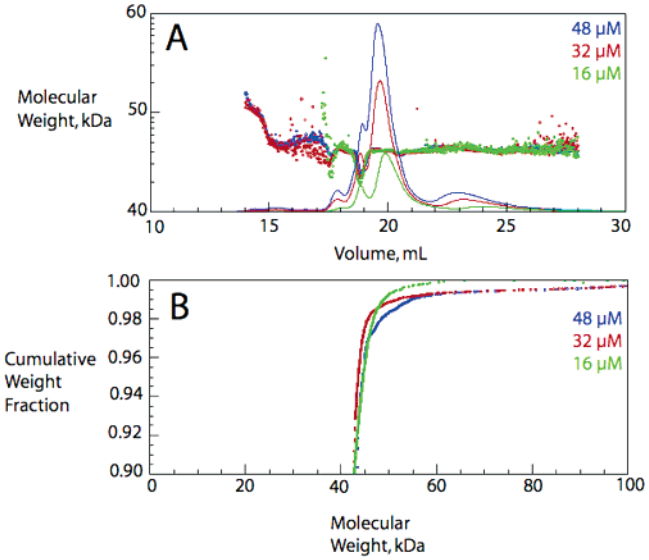

FIGURE 6: ERK2 light scattering experiments. Multiangle laser light scattering experiments were performed on three separate concentrations of active ERK2 (16, 32, and 48 μM). These values represent the concentrations of the protein injected onto the column, which eluted at concentrations (at the maximum of each peak) of 1.4, 2.9, and 3.4 μM, respectively. (A) Molar mass distribution as a function of elution volume for each sample. (B) Analysis of the cumulative molar mass distribution for each sample.

Scheme 2: Binding of a Fluorescent Ligand, L*, to ERK2, E

$$E + L^* \underset{}{\overset{[L^*]}{\rightleftharpoons}} E{\bullet}L^*$$

Table 1: Binding of Peptide and Protein Ligands to ERK2 at pH 7.5 and 27 °C

ligand	K_d for activated ERK2 (μM)	K_d for unactivated ERK2 (μM)	ligand displaced
EtsΔ138-C99*	4.7 ± 0.6[a]	1.3 ± 0.1[a]	none
EtsΔ138-C31*	2.2 ± 0.2[a]	0.7 ± 0.1[a]	none
ElkΔ138	6.0 ± 0.5[b]	1.4 ± 0.1	EtsΔ138-C31*
Elk-1 D-site[c]	2.5 ± 0.3[b]	3.9 ± 0.7[b]	EtsΔ138-C31*
Elk-1 F-site[d]	35.0 ± 3.6[b,e]	not observed[f]	EtsΔ138-C31*

[a] Determined by the binding of EtsΔ138-C31* or EtsΔ138-C99* to ERK2. [b] Determined by the displacement of EtsΔ138-C31* from ERK2. [c] The Elk-1 D-site has the sequence N-QKGKPRDLELPLSPSL-C. [d] The Elk-1 F-site has the sequence N-AKLSFQFPS-C. [e] Only 50% of the theoretical change in anisotropy observed with the addition of 150 μM peptide. [f] No change in anisotropy detected with the addition of up to 150 μM peptide.

Activated and Unactivated ERK2 Bind Ets-1 with Comparable Affinity. On the basis of the analysis given above, we assume the binding model shown in Scheme 2. When the data are fit to eq 2, dissociation constants (K_d) of 2.2 ± 0.2 and 0.7 ± 0.1 μM were obtained for the binding of EtsΔ138-C31* to activated and unactivated ERK2, respectively (Figure 5A), while EtsΔ138-C99* was found to bind activated and unactivated ERK2 with dissociation constants of 4.7 ± 0.6 and 1.3 ± 0.1 μM, respectively (Figure 5B and Table 1). In addition to determining the dissociation constant of a fluorophore-labeled protein, fluorescence anisotropy can be used to examine the binding of nonlabeled proteins to ERK2. In a competition assay, an unlabeled protein is

Scheme 3: Competition of a Nonfluorescent Ligand, L, with a Fluorescent Ligand, L*, for the Binding to ERK2[a]

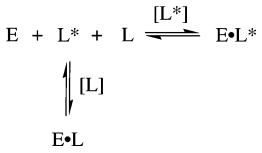

[a] It is assumed that the binding of L to ERK2 excludes the binding of L*.

allowed to compete with EtsΔ138-C31* for binding to ERK2 according to Scheme 3. Increasing the concentration of a competitor (L) therefore decreases the amount of the slowly rotating ERK2-bound EtsΔ138-C31* (E·L*), resulting in a decrease in the observed anisotropy of the solution.

A solution containing a fixed concentration of EtsΔ138-C31* and active ERK2 was added to a solution containing varied concentrations of EtsΔ138. As expected, there is a decrease in the final anisotropy reading with increasing concentrations of EtsΔ138, indicating that EtsΔ138 competes with EtsΔ138-C31* for binding to active ERK2[7] (Figure 7A). Fitting of the data to eqs 3−7 gives a dissociation constant of 5.5 ± 0.5 μM for the binding of EtsΔ138 to active ERK2, which is in good agreement with those of the labeled proteins. A similar analysis yielded dissociation constants of 0.7 ± 0.1, 1.3 ± 0.1, and 1.4 ± 0.2 μM for the binding of EtsΔ138-C31*, EtsΔ138-C99*, and EtsΔ138 to unactivated ERK2, respectively (Figure 7B and Table 1).

We have shown that both activated and unactivated ERK2 are monomeric and EtsΔ138 binds the unactivated ERK2 monomer 3-fold more tightly than the activated ERK2 monomer. This suggests that the activation segment, which must bind the Thr-38-Pro-39 motif during a catalytic cycle (Figure 1), does not stabilize the ground-state binary complex, supporting the notion that the active site of ERK2, or at least the activation segment, does not mediate the recognition of Ets-1, and points to an important role for interactions extrinsic to the consensus sequence.

Importance of Interactions Extrinsic to the Active Site in the Assembly of the Complex

N-Terminus of Ets-1. Previously, it was shown that a protein comprised of residues 1−52 of Ets-1 is a good substrate for ERK2 with a k_{cat} of 9 s^{-1} and a K_m^{ets} of 190 μM (*31*). This result is interesting because it suggests that these residues bind ERK2 with an affinity higher than what would be expected if the consensus sequence mediated binding alone.[8] This K_m^{ets} value is similar to the dissociation constant (K_d^{ets}) of 30 ± 20 μM that we determined using the competition assay (Table 2). A free energy of binding ($\Delta G°$) of −26 kJ/mol at 298 K may be estimated, which is comparable to the $\Delta G°$ for EtsΔ138, and presumably the full-length protein also (Figure 8). As this suggests that the N-terminus of Ets-1 contributes to the stabilization of the ternary complex, we examined the binding further and deleted residues 1−23 from EtsΔ138 to give a new protein, EtsΔ24−138 (Scheme 1). Using the competition assay, we found that the deletion weakened the affinity of EtsΔ138 for activated ERK2 by 12-fold (Table 2). Using the same assay, we found that a further deletion of residues 24−50, which includes the φ-χ-Ser/Thr-Pro sequence, resulted in only an additional 1.5-fold decrease in the affinity of the complex (Table 2), supporting the notion that the contribution from the consensus sequence is minimal. This species, EtsΔ51−138, is comprised essentially of just the PNT domain and binds with a dissociation constant of 129 μM,

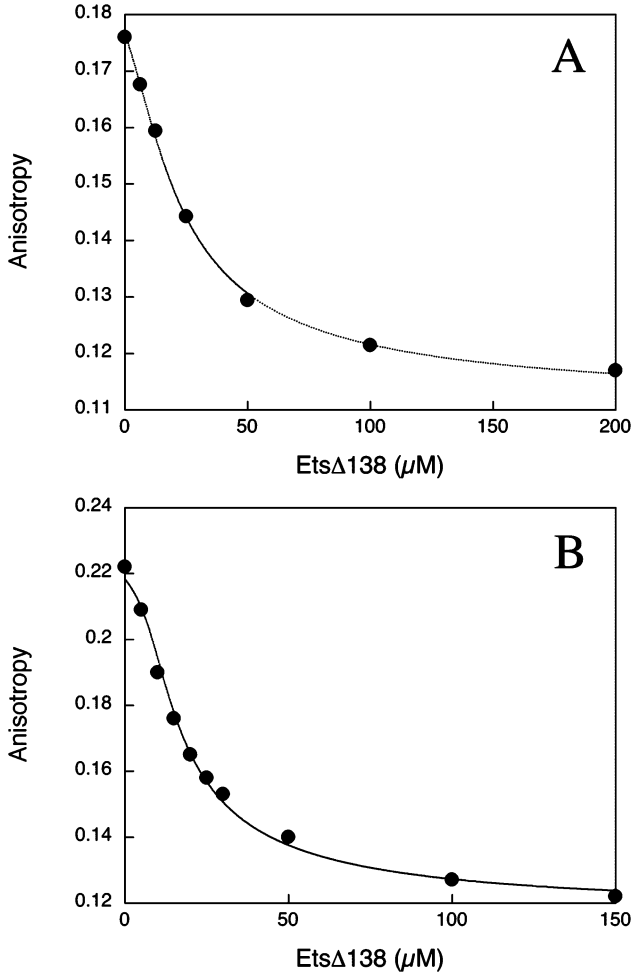

FIGURE 7: Fluorescence anisotropy competition assay for assessing the binding of EtsΔ138 to ERK2. Each assay contained 100 nM EtsΔ138-C31*, 0−150 μM EtsΔ138, and 10 μM active ERK2 (A) or 9.55 μM inactive ERK2 (B). Experimental data were plotted and fit to eqs 3−7 using an R value of 0.5 and a K_d value of 2.2 μM (active ERK2) or 0.7 μM (inactive ERK2). The K_d values were established from previously performed fluorescence anisotropy assays that examined the binding of EtsΔ138-C31* to active or inactive ERK2.

Table 2: Binding of EtsΔ138 to ERK2 at pH 7.5 and 27 °C

	K_d[a] (μM)		K_d[a] (μM)
EtsΔ138	6.6 ± 1.2	EtsΔ138 Pro-39Val	8.8 ± 0.3
ΔHisEtsΔ138	10.0 ± 0.1	EtsΔ138 Pro-39Gly	7.9 ± 0.5
EtsΔ1−52	30.0 ± 20	EtsΔ138 Pro-39Arg	4.9 ± 0.8
EtsΔ24−138	83.0 ± 3	EtsΔ138 Pro-39Asp	8.0 ± 0.5
EtsΔ51−138	130 ± 7	EtsΔ138 Pro-39Glu	11.0 ± 0.8
EtsΔ138 Pro-39Ala	8.0 ± 0.5	EtsΔ138 Phe-120Ala	68.0 ± 5.0

[a] Determined by the displacement of EtsΔ138-C31* from activated ERK2.

[7] Bovine serum albumin was used as a nonspecific protein competitor and did not dissociate the ERK2·EtsΔ138* complex with concentrations of up to 200 μM.

[8] Peptides containing consensus sequences are generally poor substrates for MAP kinases (*42*), and the peptide KKK-EtsΔ33−43 is not effectively phosphorylated by ERK2 (M. Rainey, unpublished observations).

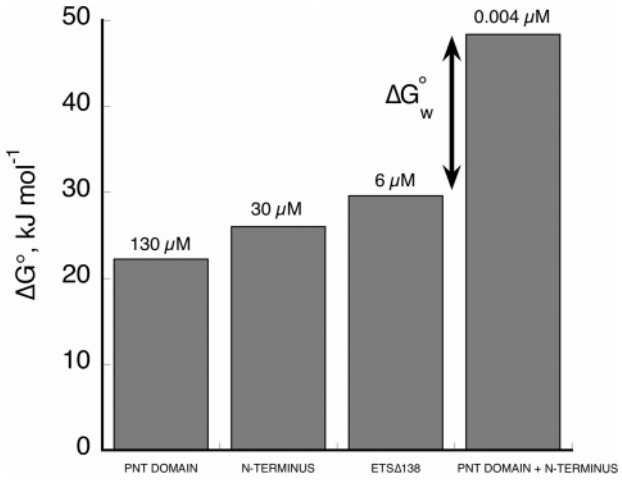

FIGURE 8: Contribution of the two docking sites on Ets-1 to the free energy of binding to ERK2. EtsΔ51−138 (corresponds to the PNT domain), EtsΔ1−52 (corresponds to the N-terminus), and EtsΔ138 bind activated ERK2 with dissociation constants of 130, 30, and 6 μM, respectively. Full expression of the binding of the two domains predicts that EtsΔ138 would bind with a dissociation constant in the region of 4 nM.

which is similar to the affinity of the N-terminal domain (EtsΔ1−52) (Table 2) (see Scheme 1 for an illustration of constructs).

Thus, the picture that emerges is one in which two docking sites in EtsΔ138 contribute equally to the stability of the assembled complex, in contrast to the consensus sequence, φ-χ-Ser/Thr-Pro, which does not appear to make a significant contribution. The regions of Ets-1 (EtsΔ1−52 and EtsΔ51−128) are estimated to bind ERK2 with free energies of −26 and −22 kJ/mol, respectively,[9] while EtsΔ138 binds with a slightly higher affinity ($\Delta G^\circ = -30$ kJ/mol). Interestingly, the binding energy from the two docking sites is not fully expressed in the binding of EtsΔ138, suggesting that a small cost (ΔG^o_w) is associated with simultaneously binding both domains (Figure 8). The full expression of the binding would result in a significantly more stable complex, with a dissociation constant (K_d) of 4 nM. The 12-fold decrease in affinity, as a result of the deletion of the first 23 amino acids, to give EtsΔ24−138, suggests that a site adjacent to or within the first 23 residues of Ets-1 helps tether the ERK2·Ets-1 complex. These data support the notion that the N-terminus of Ets-1 may become more ordered upon formation of the complex.

Substrate-Binding Groove. The structures of several protein kinases have been determined as complexes with either a peptide substrate or a peptide inhibitor (*19*). These structures reveal that important interactions are often mediated by the substrate-binding groove. In ERK2, the substrate-binding groove may be considered to be comprised of residues in loop 13, the αD helix, loop 8, and the αG helix as well as several residues within and following the C-terminus of the MAPK insert (see Figure 1). Recently, in an extensive mutational analysis, Zhang's laboratory showed that ERK2 utilizes this substrate-binding groove to bind transcription factor Elk-1 (*43*), while earlier studies on p38 MAPK (*44*) and JNK (*26*) also implicated this region in substrate binding. We were interested in determining whether Ets-1 binds in this groove also, but rather than perform an extensive mutational analysis, we chose to focus on a pair of residues in loop 13 that may have evolved to distinguish ERK2 from other MAPKs (*45*). Consequently, Lys-229 and His-230, which lie in loop 13, were mutated to Thr and Asp, respectively (the corresponding residues in p38 MAPKα), to give the Lys-229Thr/His-230Asp mutant. When the binding of EtsΔ138-C31* to the unactivated ERK2 mutant was examined, binding was found to be compromised 40-fold (data not shown), suggesting that indeed Ets-1 binds in the substrate-binding groove.

Recruitment Sites. The mechanism by which ERK2 utilizes the D- and F-recruitment sites has not been studied in detail. The D-recruitment site is comprised of the β7−β8 reverse turn and the αD−αE helix and flanks one side of the substrate-binding groove (*46*). The F-recruitment site comprises part of the activation segment starting at Phe-181 to the end of loop 12 (Phe-181−Thr-204), the αG helix (Tyr-231−Leu-242), and the MAPK insert α2L14 helix (Leu-256−Leu-263) (Figure 1) (*24*). While both sites have been shown to improve the specificity of substrate phosphorylation (*20*−*22*, *47*), much needs to be done to understand the nature and the specificity of these interactions.

As Phe-120 is important for ERK2 binding, we were curious to see whether the Elk-1-derived peptide N-AKLS-FQFPS-C (*21*), which binds in the F-recruiting site (*24*), might compete with EtsΔ138-C31* for binding to activated ERK2. To examine this, we utilized the competition binding assay to determine whether the peptide could displace EtsΔ138-C31* from ERK2. The decrease in anisotropy, shown in Figure 9A, suggests that it can, and an analysis of the data according to eqs 3−7 gives an apparent K_d of 35 ± 5 μM for the peptide (Table 1). Notably, the addition of the peptide to the ERK2·EtsΔ138-C31* complex containing inactive ERK2 resulted in no decrease in anisotropy, consistent with the notion that the peptide fails to bind unactivated ERK2 (Figure 9B). Thus, despite the fact that Ets-1 does not require the F-recruitment site to bind ERK2, it is displaced from ERK2 by the F-site peptide. We also tested whether the D-site peptide from Elk-1 [Elk-1-DEJL, N-QKGKPRDLELPLSPSLR-C (*25*)] could compete with EtsΔ138-C31*. In contrast to the F-site peptide, the D-site peptide competed with EtsΔ138-C31* for binding to both the activated and unactivated ERK2 (Figure 10A,B). Fitting of the data established dissociation constants (K_d) of 2.5 ± 0.3 and 3.9 ± 0.2 μM for active and unactivated ERK2, respectively (Table 1). In summary, despite the fact that Ets-1 does not contain a recognizable D- or F-site, peptides derived from these docking sites displace Ets-1 from ERK2, consistent with the notion that Ets-1 communicates to both the D- and F-recruitment sites on ERK2.

Unimportance of Interactions Intrinsic to the Active Site in the Assembly of the Complex

We took advantage of the competition assay to examine the role the $^{36}\varphi$-χ-Thr-Pro^{39} sequence might play in complex assembly. We focused on Pro-39 and mutated it to several different amino acids, which have steric and electrostatic properties very different from those of proline. Surprisingly,

[9] It should be noted that the while the φ-χ-Ser/Thr-Pro sequence does not appear to contribute to the stability of EtsΔ138, we cannot rule out the possibility that it does not contribute to the binding of EtsΔ1−52.

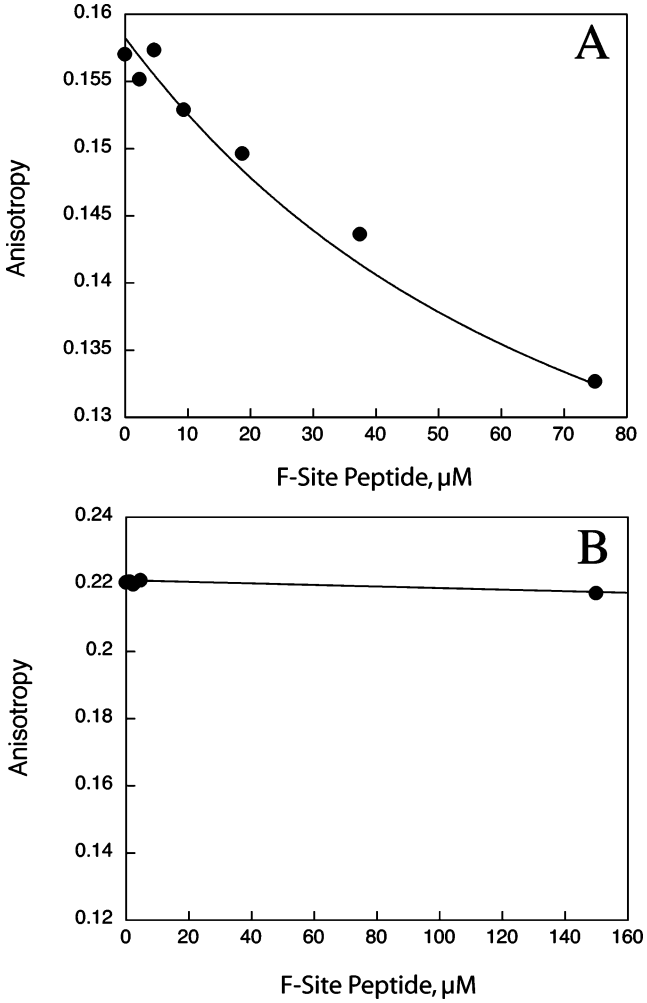

FIGURE 9: Fluorescence anisotropy competition assay for assessing binding of the Elk-1 F-site peptide to ERK2. Each assay contained 100 nM EtsΔ138-C31*, 0−150 μM F-site peptide, and 5 μM active ERK2 (A) or inactive ERK2 (B). Experimental data were plotted and fit to eqs 3−7 using an R value of 0.5 and a K_d value of 2.2 μM (active ERK2) or 0.7 μM (inactive ERK2). The K_d values were established from previously performed fluorescence anisotropy assays that examined the binding of EtsΔ138-C31* to active or inactive ERK2.

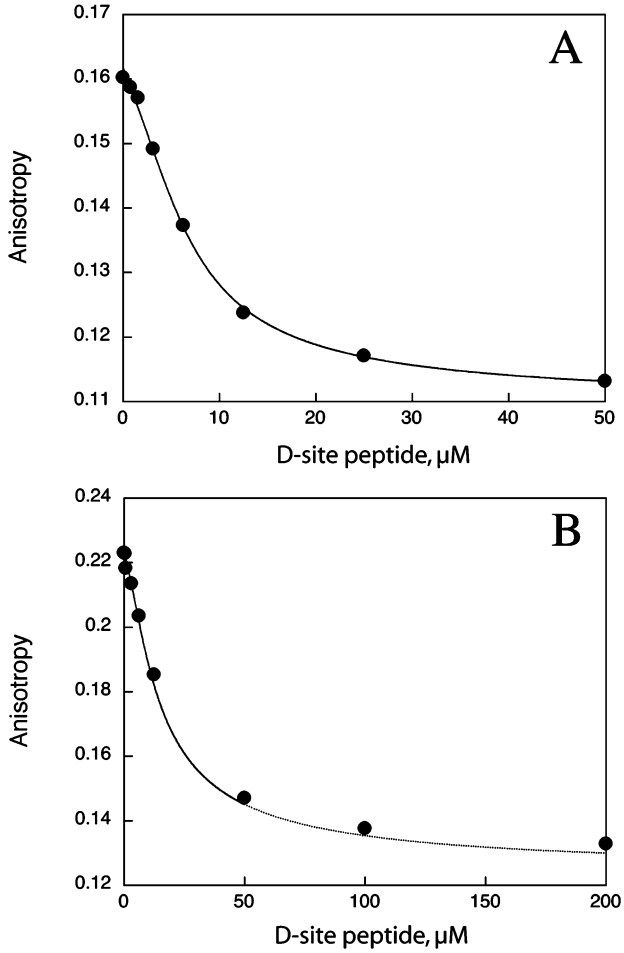

FIGURE 10: Fluorescence anisotropy competition assay for assessing the binding of the Elk-1 D-site peptide to ERK2. Each assay contained 100 nM EtsΔ138-C31*, 0−200 μM D-site peptide, and 5 μM active ERK2 (A) or inactive ERK2 (B). Experimental data were plotted and fit to eqs 3−7 using an R value of 0.5 and a K_d value of 2.2 μM (active ERK2) or 0.7 μM (inactive ERK2). The K_d values were established from previously performed fluorescence anisotropy assays that examined the binding of EtsΔ138-C31* to active or inactive ERK2.

the mutants exhibited very little variation in the dissociation constant (K_d) (Table 2).[10] This result is interesting because it is presumed that Pro-39 must bind the P+1 pocket (Figure 2) during the transition state for phosphoryl transfer. The incorporation of non-proline amino acids in the P+1 position is expected to severely destabilize the binding of the consensus sequence, because not only is binding within the P+1 pocket likely to be disrupted but the integrity of the interaction of Thr-38 with the P0 site is likely to be affected also. Furthermore, while the effect of mutating the P+1 proline will not necessarily extend as far as the P−2 binding pocket, this is a low-specificity pocket that probably does not offer substantial stabilization to the binding of a substrate.[8]

Structural studies on protein kinase A (PKA) bound to the inhibitor peptide, PKI, and Mn_2ATP^{2-} show the protein kinase domain in a conformation that is more closed and compact than the uncomplexed kinase (*48*). Therefore, we were interested in seeing whether we could detect whether ERK2 formed a compact structure with both substrates bound. In this case, we reasoned that a bound ATP analogue would increase the affinity of EtsΔ138 for activated ERK2. As ERK2 is activated by a second Mg^{2+} ion that binds with a dissociation constant of approximately 2−5 mM in the presence of ATP (*16*), we performed experiments in the presence of 20 mM Mg^{2+} to ensure that two Mg^{2+} ions were bound to the enzyme. The binding data (Table 3) show that EtsΔ138 binds activated ERK2 approximately 5 times more weakly than in the absence of Mg^{2+}. The mechanism by which Mg^{2+} destabilizes the binding of EtsΔ138 is unclear but could be related to the binding of the second "activating" Mg^{2+} ion to ERK2 (*16*). Notably, AMP-PNP has no affect on the affinity of EtsΔ138, or the EtsΔ138 ThrPro/AlaAla mutant, for ERK2 in the presence of 20 mM Mg^{2+}, suggesting that the two substrates do not interact synergistically to form a more stable complex, and argues against the formation of a closed ternary complex (Table 3). This is

[10] All the mutants, including the double mutant EtsΔ138 Thr-38Ala/Pro-39Ala, exhibit dissociation constants that are within 50% of the mean value of 8 μM (Table 2).

[11] Residues Thr-157 and Thr-158 have been called the ED-domain, named after the corresponding Asp and Glu residues found in p38 MAPKα.

Table 3: Affinity of ERK2 and EtsΔ138 in Magnesium Solutions

protein	[Mg^{2+}] (free) (mM)	[AMP-PNP] (mM)	K_d (μM)
EtsΔ138	20	0	29 ± 13^a
EtsΔ138	20	2	29 ± 2^a
EtsΔ138	2	0	5.2 ± 0.5
EtsΔ138	2	2	9.0 ± 1.6
EtsΔ138	0	0	6.6 ± 1.2^a
EtsΔ138 T38A/P39A	20	0	51 ± 4^a
EtsΔ138 T38A/P39A	20	2	58 ± 6^a
EtsΔ138 T38A/P39A	0	0	11 ± 1^a

[a] Determined by the displacement of EtsΔ138-C31* from ERK2.

consistent with previous steady-state kinetic data and is consistent with the notion that the lowest-energy form of the ternary complex occurs without the participation of the activation segment of the enzyme (*18*).

DISCUSSION

Absence of Self-Association of Activated ERK2. It has been suggested that ERK2 can self-associate in solution, by interactions between residues on loop 16 and helix αL16 (*9*). We were surprised by the relative amplitudes of the binding curves in Figure 5 as they suggested that activated ERK2 was not a dimer. Therefore, we decided to determine the oligomerization state of the activated enzyme and subjected three different concentrations of activated ERK2 to gel filtration (Figure 6A). Fractions of the eluted protein were subjected to multiangle laser light scattering analysis. Classical light scattering measures the intensity of light scattered by a solution at some angle relative to the incident laser beam. The measured intensity is directly proportional to the molar mass of the protein multiplied by the concentration (milligrams per milliliter). Therefore, the measured intensity together with the signal from a concentration detector (refractive index or absorbance) can be used to calculate the molar mass of each peak coming off the column. The molecular masses derived by this technique are generally accurate within 3% or better. The analysis in Figure 6B shows that ~99% of the eluted protein has a calculated mass of <45 kDa. The chromatogram shows four distinct peaks at elution volumes of ~18, ~19, ~20, and ~23 mL (Figure 6A). Previously published profiles (*9*) are similar to those reported here. The nature of the protein at an elution volume of ~19 mL with a molar mass of ~22 kDa is unknown. The protein of each of the other fractions has a weight-average molar mass of 41.2 ± 0.2 kDa compared to the expected mass of 42.3 kDa. This finding shows that activated ERK2 does not self-associate under the conditions of our binding experiments.

Other studies have also failed to establish the self-association of activated ERK2. For example, cross-linking agents were relatively inefficient at cross-linking an 8 μM solution of ERK2 but could efficiently cross-link ERK2 and MKP3 (*49*). In another study, no evidence of ERK2 self-association was found using FRET methods (*50*). In contrast, a FRET signal was detected between MKK1 and ERK2 (*50*). Some studies are inconclusive on the matter. For example, ERK2 shows a decreased rate of H−D exchange in loop 16, upon activation (*51*), which could be the result of self-association; however, protection due to the structural transition from loop to helix that is seen to accompany the activation in the crystal structure, and not protection by the homodimer interface, cannot be ruled out. We found a small hyperbolic variation in k_{cat} of 20−37 s^{-1}, for the phosphorylation of EtsΔ138, when the ERK2 concentration was varied from 0.002 to 5 μM, which was consistent with the self-association of ERK2 (*17*). One possible explanation for this observation is that under the conditions of the experiment the binding of excess EtsΔ138 promoted the self-association of ERK2, by altering its conformation. It should be noted that we cannot rule out the possibility that differences in the oligomerization state of the enzyme reflect differences in the methods of its preparation. For example, Khokhlatchev et al. prepared activated ERK2 by coexpression with an active MKK1 (*9*), whereas in the study presented here, the unactivated enzyme was first isolated after overexpression and then activated by MKK1 in vitro. In summary, while ERK2 may have a propensity to self-associate, under some conditions (*9*), it does not appear to be an obligate result of activation and is not significant in the assays presented here.

Absence of Regulation by Protein Phosphorylation. To investigate how ERK2 recognizes Ets-1, we examined the effect of ERK2's activation state on its ability to bind EtsΔ138 (Figures 5 and 7). Activation of ERK2 by MKK1 requires the phosphorylation of two residues, Thr-183 and Tyr-185, whose phosphorylation stabilizes the remodeling of the activation segment (Figure 1) (*52*). This remodeling realigns the active site and forms the P+1 Pro binding pocket (Figure 2). However, despite this, EtsΔ138 binds unactivated ERK2 3-fold more tightly than activated ERK2 (Figure 5 and Table 1), indicating that the orientation of the activation loop is not critical for EtsΔ138 binding. Ets-1 is not the only substrate to bind the unactivated form of the enzyme as p90RSK does also (*53*). It seems that a substrate consensus sequence, φ-χ-Ser/Thr-Pro, may not necessarily contribute to the stability of a number of ERK2·substrate (or even ERK2·product) complexes. This opens up the intriguing possibility that many other substrates of ERK2 also bind the unactivated form of ERK2, thus contributing to its localization and regulation. This is particularly likely since the unactivated enzyme binds a D-site peptide (Figure 10), and a relatively small change occurs in the structure of the substrate-binding groove as well as the MAPK insert, upon activation of ERK2 (Figure 1).

While it is often assumed in the literature that protein kinases form tight complexes with protein substrates, it is likely that their affinities vary over a range, reflecting the precise physiological function of each complex. Although the dissociation constants measured here for the ERK2·Ets-1 complexes are relatively weak, probably falling significantly above the concentration of Ets-1 in a cell, they are similar to the strength of the interactions of MAPKs with other proteins. To fully understand the function of ERK2 in cells, further work is required to address issues such as macromolecular and molecular crowding that can contribute significantly to both diffusional processes and the stability of protein complexes (*54*).

Evidence for Two Docking Sites in Ets-1 that Bind ERK2. As shown in Figure 8, both the N-terminus and the PNT domain of Ets-1 (Figure 3) contribute to the affinity of EtsΔ138. The consensus sequence, $^{36}\varphi$-χ-Thr-Pro^{39}, is not important. EtsΔ138-C31* undergoes a change in fluorescence yield upon binding both activated and unactivated ERK2

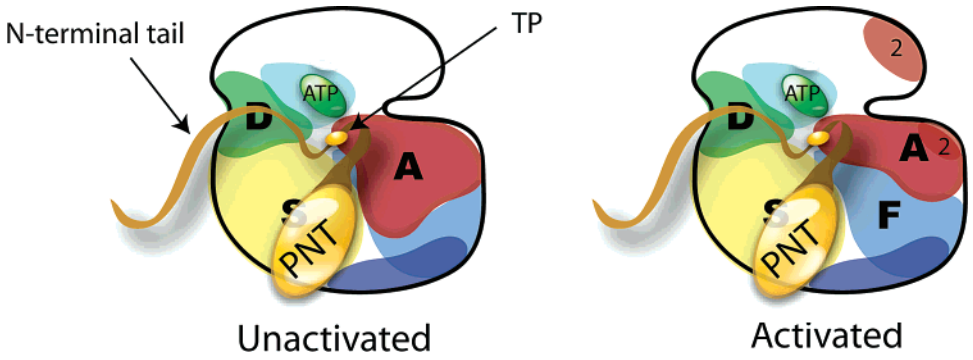

FIGURE 11: Schematic representation of the ERK2·EtsΔ138 complex showing how EtsΔ138 might bind to ERK2. The color scheme corresponds to the color scheme in Figure 1, and the characters D, F, S, A, and 2 correspond to the D-recruitment site, the F-recruitment site, the substrate-binding groove, the activation segment, and the crystallographic dimer interface, respectively.

(Figure 4), indicating that, in both cases, the fluorescein experiences a similar change in environment upon binding ERK2. The data in Table 2 suggest that the binding of the N-terminus appears to stem from interactions associated with the first 23 residues of Ets-1, indicating that the highly flexible N-terminal tail becomes organized and contains a weak and previously unrecognized docking site for ERK2.

How then does Ets-1 bind ERK2? One intriguing possibility is that the N-terminal tail binds the D-recruitment site of ERK2, while the PNT domain binds the substrate-binding groove (see Figure 11). While remaining to be proven, this model is attractive for a number of reasons. It is consistent with the observation that EtsΔ138 is displaced from ERK2 by the D-site peptide (Figure 10), which would compete with the N-terminal tail for binding to ERK2 and explains why a mutation in loop 13 of the substrate-binding groove destabilizes the complex. Another feature of the model is that it places the consensus motif in the correct orientation for binding to the activation segment in the transition state for phosphoryl transfer.

The H−D exchange analysis of Lee et al. revealed changes in exchange rate, upon D-site peptide binding, which were localized to the D-recruitment site (*24*). In addition, a slight increase in the exchange rate was also seen in the activation segment, which is consistent with the apparent communication between the two loci that is seen in two recent crystal structures (*55*, *56*). Significantly, however, the binding of Ets-1 is insensitive to the conformation of this segment (Figure 5 and Table 1), suggesting that for the D-site peptide to displace Ets-1 they most likely share a common binding site. According to the schematic model in Figure 11, Ets-1 binds both activated and unactivated ERK2 in a similar manner, where its loop which is between the two docking sites adopts a conformation in which the consensus sequence is near but not physically engaged with the activation segment.

This model, where the phosphorylation site is tethered in the proximity of the active site, provides the basis for understanding other MAPK−substrate interactions and is reminiscent of the mechanism of substrate recognition by another promiscuous enzyme, thrombin (*57*). This mechanism also provides an explanation about why Ser-26 is not phosphorylated.

It is unclear why the F-site peptide displaces Ets-1 from ERK2 as Ets-1 does not possess an F-site and EtsΔ138 does not bind the F-recruiting site, which is only present in the activated enzyme (Figure 9). It remains to be seen whether this interaction is steric or allosteric in nature. The binding of the F-site peptide certainly induces long-range changes in the H−D exchange rate (*51*), suggesting that the latter mechanism is quite possible.

Role of Weak Docking Sites and Anticooperativity. The general topology of the model in Figure 11 may be similar to that of other MAPK−protein interactions, because several proteins are known to possess a docking site in an either N- or C-terminal tail. Both MAPKK1 (*58*, *59*) and MAPKAP-K2 (*60*), for example, are recruited to ERK2 and p38 MAPK, respectively, by D-sites, which are thought to be in relatively flexible tails that lie at the ends of the proteins. Similarly, PEA-15 contains an important docking site at the end of a flexible tail (*61*). While the N-terminus of Ets-1 is not highly conserved, there is similarity with the N-terminus of Ets-2, which is another substrate of ERK2 (see Figure 3B for a comparison of the sequences). This is consistent with the notion that a docking site with a low specificity is conserved in both proteins. According to the model, the binding of the PNT domain serves as a specificity element that helps position the N-terminus for the appropriate interactions. Notably, an anticooperative mode of binding might facilitate the transient formation of the complex and ensure that the release of the phosphorylated product is relatively fast. It will be interesting to examine the rates of complex assembly in the context of the proposed model.

ACKNOWLEDGMENT

We are indebted to Dr. Melanie Cobb (University of Texas Southwestern Medical Center, Dallas, TX) and Dr. Natalie G. Ahn (University of Colorado, Boulder, CO) for generously providing us with DNA encoding His_6-ERK2 and His_6-MKK1G7B, respectively. We thank Dr. Walter Fast (University of Texas) for critical comments on a previous version of the manuscript.

SUPPORTING INFORMATION AVAILABLE

Expression and purification of MKK1G7B, ERK2, and EtsΔ138, activation of ERK2 by MKK1G7B, site-directed mutagenesis, preparation of fluorescein-labeled EtsΔ138, and derivation of equations. This material is available free of charge via the Internet at http://pubs.acs.org.

REFERENCES

1. Mor, A., and Philips, M. R. (2006) Compartmentalized Ras/MAPK Signaling, *Annu. Rev. Immunol.* (in press).

2. Yoon, S., and Seger, R. (2006) The extracellular signal-regulated kinase: Multiple substrates regulate diverse cellular functions, *Growth Factors 24*, 21−44.
3. Rubinfeld, H., and Seger, R. (2005) The ERK cascade: A prototype of MAPK signaling, *Mol. Biotechnol. 31*, 151−74.
4. MacCorkle, R. A., and Tan, T. H. (2005) Mitogen-activated protein kinases in cell-cycle control, *Cell Biochem. Biophys. 43*, 451−61.
5. Chuderland, D., and Seger, R. (2005) Protein-protein interactions in the regulation of the extracellular signal-regulated kinase, *Mol. Biotechnol. 29*, 57−74.
6. Dunn, K. L., Espino, P. S., Drobic, B., He, S., and Davie, J. R. (2005) The Ras-MAPK signal transduction pathway, cancer and chromatin remodeling, *Biochem. Cell Biol. 83*, 1−14.
7. Morrison, D. K., and Davis, R. J. (2003) Regulation of MAP kinase signaling modules by scaffold proteins in mammals, *Annu. Rev. Cell Dev. Biol. 19*, 91−118.
8. Pearson, G., Robinson, F., Beers Gibson, T., Xu, B. E., Karandikar, M., Berman, K., and Cobb, M. H. (2001) Mitogen-activated protein (MAP) kinase pathways: Regulation and physiological functions, *Endocr. Rev. 22*, 153−83.
9. Khokhlatchev, A. V., Canagarajah, B., Wilsbacher, J., Robinson, M., Atkinson, M., Goldsmith, E., and Cobb, M. H. (1998) Phosphorylation of the MAP kinase ERK2 promotes its homodimerization and nuclear translocation, *Cell 93*, 605−15.
10. Hutti, J. E., Jarrell, E. T., Chang, J. D., Abbott, D. W., Storz, P., Toker, A., Cantley, L. C., and Turk, B. E. (2004) A rapid method for determining protein kinase phosphorylation specificity, *Nat. Methods 1*, 27−9.
11. Gonzalez, F. A., Raden, D. L., and Davis, R. J. (1991) Identification of substrate recognition determinants for human ERK1 and ERK2 protein kinases, *J. Biol. Chem. 266*, 22159−63.
12. Alvarez, E., Northwood, I. C., Gonzalez, F. A., Latour, D. A., Seth, A., Abate, C., Curran, T., and Davis, R. J. (1991) Pro-Leu-Ser/Thr-Pro is a consensus primary sequence for substrate protein phosphorylation. Characterization of the phosphorylation of c-myc and c-jun proteins by an epidermal growth factor receptor threonine 669 protein kinase, *J. Biol. Chem. 266*, 15277−85.
13. Nolen, B., Taylor, S., and Ghosh, G. (2004) Regulation of protein kinases: Controlling activity through activation segment conformation, *Mol. Cell 15*, 661−75.
14. Waas, W. F., and Dalby, K. N. (2001) Purification of a model substrate for transcription factor phosphorylation by ERK2, *Protein Expression Purif. 23*, 191−7.
15. Waas, W. F., and Dalby, K. N. (2002) Transient protein-protein interactions and a random-ordered kinetic mechanism for the phosphorylation of a transcription factor by extracellular-regulated protein kinase 2, *J. Biol. Chem. 277*, 12532−40.
16. Waas, W. F., and Dalby, K. N. (2003) Physiological concentrations of divalent magnesium ion activate the serine/threonine specific protein kinase ERK2, *Biochemistry 42*, 2960−70.
17. Waas, W. F., Rainey, M. A., Szafranska, A. E., and Dalby, K. N. (2003) Two rate-limiting steps in the kinetic mechanism of the serine/threonine specific protein kinase ERK2: A case of fast phosphorylation followed by fast product release, *Biochemistry 42*, 12273−86.
18. Rainey, M. A., Callaway, K., Barnes, R., Wilson, B., and Dalby, K. N. (2005) Proximity-Induced Catalysis by the Protein Kinase ERK2, *J. Am. Chem. Soc. 127*, 10494−5.
19. Kemp, B. E., Parker, M. W., Hu, S., Tiganis, T., and House, C. (1994) Substrate and pseudosubstrate interactions with protein kinases: Determinants of specificity, *Trends Biochem. Sci. 19*, 440−4.
20. Sharrocks, A. D., Yang, S. H., and Galanis, A. (2000) Docking domains and substrate-specificity determination for MAP kinases, *Trends Biochem. Sci. 25*, 448−53.
21. Jacobs, D., Glossip, D., Xing, H., Muslin, A. J., and Kornfeld, K. (1999) Multiple docking sites on substrate proteins form a modular system that mediates recognition by ERK MAP kinase, *Genes Dev. 13*, 163−75.
22. Fantz, D. A., Jacobs, D., Glossip, D., and Kornfeld, K. (2001) Docking sites on substrate proteins direct extracellular signal-regulated kinase to phosphorylate specific residues, *J. Biol. Chem. 276*, 27256−65.
23. MacKenzie, S. J., Baillie, G. S., McPhee, I., Bolger, G. B., and Houslay, M. D. (2000) ERK2 mitogen-activated protein kinase binding, phosphorylation, and regulation of the PDE4D cAMP-specific phosphodiesterases. The involvement of COOH-terminal docking sites and NH_2-terminal UCR regions, *J. Biol. Chem. 275*, 16609−17.
24. Lee, T., Hoofnagle, A. N., Kabuyama, Y., Stroud, J., Min, X., Goldsmith, E. J., Chen, L., Resing, K. A., and Ahn, N. G. (2004) Docking motif interactions in MAP kinases revealed by hydrogen exchange mass spectrometry, *Mol. Cell 14*, 43−55.
25. Yang, S. H., Whitmarsh, A. J., Davis, R. J., and Sharrocks, A. D. (1998) Differential targeting of MAP kinases to the ETS-domain transcription factor Elk-1, *EMBO J. 17*, 1740−9.
26. Kallunki, T., Su, B., Tsigelny, I., Sluss, H. K., Derijard, B., Moore, G., Davis, R., and Karin, M. (1994) JNK2 contains a specificity-determining region responsible for efficient c-Jun binding and phosphorylation, *Genes Dev. 8*, 2996−3007.
27. Yang, S. H., Galanis, A., and Sharrocks, A. D. (1999) Targeting of p38 mitogen-activated protein kinases to MEF2 transcription factors, *Mol. Cell. Biol. 19*, 4028−38.
28. Graves, B. J., and Petersen, J. M. (1998) Specificity within the ets family of transcription factors, *Adv. Cancer Res. 75*, 1−55.
29. Bartel, F. O., Higuchi, T., and Spyropoulos, D. D. (2000) Mouse Models in the Study of the Ets Family of Transcription Factors, *Oncogene 19*, 6443−654.
30. Foulds, C. E., Nelson, M. L., Blaszczak, A. G., and Graves, B. J. (2004) Ras/mitogen-activated protein kinase signaling activates Ets-1 and Ets-2 by CBP/p300 recruitment, *Mol. Cell. Biol. 24*, 10954−64.
31. Seidel, J. J., and Graves, B. J. (2002) An ERK2 docking site in the Pointed domain distinguishes a subset of ETS transcription factors, *Genes Dev. 16*, 127−37.
32. Callaway, K., Rainey, M. A., and Dalby, K. N. (2005) Quantifying ERK2-protein interactions by fluorescence anisotropy: PEA-15 inhibits ERK2 by blocking the binding of DEJL domains, *Biochim. Biophys. Acta 1754*, 316−23.
33. Kholodenko, B. N., Brown, G. C., and Hoek, J. B. (2000) Diffusion control of protein phosphorylation in signal transduction pathways, *Biochem. J. 350* (Part 3), 901−7.
34. Kholodenko, B. N. (2000) Negative feedback and ultrasensitivity can bring about oscillations in the mitogen-activated protein kinase cascades, *Eur. J. Biochem. 267*, 1583−8.
35. Schoeberl, B., Eichler-Jonsson, C., Gilles, E. D., and Muller, G. (2002) Computational modeling of the dynamics of the MAP kinase cascade activated by surface and internalized EGF receptors, *Nat. Biotechnol. 20*, 370−5.
36. Mayawala, K., Gelmi, C. A., and Edwards, J. S. (2004) MAPK cascade possesses decoupled controllability of signal amplification and duration, *Biophys. J. 87*, L01−2.
37. Bhalla, U. S. (2004) Signalin in Small Subcellular Volumes. 1. Stochastic and Diffusion Effects on Individual Pathways, *Biophys. J. 87*, 733−44.
38. Orton, R. J., Sturm, O. E., Vyshemirsky, V., Calder, M., Gilbert, D. R., and Kolch, W. (2005) Computational modelling of the receptor-tyrosine-kinase-activated MAPK pathway, *Biochem. J. 392*, 249−61.
39. Bluthgen, N., Bruggeman, F. J., Legewie, S., Herzel, H., Westerhoff, H. V., and Kholodenko, B. N. (2006) Effects of sequestration on signal transduction cascades, *FEBS Lett. 273*, 895−906.
40. Takahashi, K., Arjunan, S. N., and Tomita, M. (2005) Space in systems biology of signaling pathways: Towards intracellular molecular crowding in silico, *FEBS Lett. 579*, 1783−8.
41. Cobb, M. H., and Goldsmith, E. J. (2000) Dimerization in MAP-kinase signaling, *Trends Biochem. Sci. 25*, 7−9.
42. Hawkins, J., Zheng, S., Frantz, B., and LoGrasso, P. (2000) p38 map kinase substrate specificity differs greatly for protein and peptide substrates, *Arch. Biochem. Biophys. 382*, 310−3.
43. Zhang, J., Zhou, B., Zheng, C. F., and Zhang, Z. Y. (2003) A bipartite mechanism for ERK2 recognition by its cognate regulators and substrates, *J. Biol. Chem. 278*, 29901−12.
44. Gum, R. J., and Young, P. R. (1999) Identification of two distinct regions of p38 MAPK required for substrate binding and phosphorylation, *Biochem. Biophys. Res. Commun. 266*, 284−9.
45. Caffrey, D. R., O'Neill, L. A., and Shields, D. C. (1999) The evolution of the MAP kinase pathways: Coduplication of interacting proteins leads to new signaling cascades, *J. Mol. Evol. 49*, 567−82.
46. Chang, C. I., Xu, B. E., Akella, R., Cobb, M. H., and Goldsmith, E. J. (2002) Crystal structures of MAP kinase p38 complexed to the docking sites on its nuclear substrate MEF2A and activator MKK3b, *Mol. Cell 9*, 1241−9.

47. Barsyte-Lovejoy, D., Galanis, A., and Sharrocks, A. D. (2002) Specificity determinants in MAPK signaling to transcription factors, *J. Biol. Chem. 277*, 9896−903.
48. Zheng, J., Knighton, D. R., Xuong, N. H., Taylor, S. S., Sowadski, J. M., and Ten Eyck, L. F. (1993) Oct) Crystal structures of the myristylated catalytic subunit of cAMP-dependent protein kinase reveal open and closed conformations, *Protein Sci. 2*, 1559−73.
49. Kim, Y., Rice, A. E., and Denu, J. M. (2003) Intramolecular dephosphorylation of ERK by MKP3, *Biochemistry 42*, 15197−207.
50. Burack, W. R., and Shaw, A. S. (2005) Live Cell Imaging of ERK and MEK: Simple binding equilibrium explains the regulated nucleocytoplasmic distribution of ERK, *J. Biol. Chem. 280*, 3832−7.
51. Hoofnagle, A. N., Stoner, J. W., Lee, T., Eaton, S. S., and Ahn, N. G. (2004) Phosphorylation-dependent changes in structure and dynamics in ERK2 detected by SDSL and EPR, *Biophys. J. 86*, 395−403.
52. Canagarajah, B. J., Khokhlatchev, A., Cobb, M. H., and Goldsmith, E. J. (1997) Activation mechanism of the MAP kinase ERK2 by dual phosphorylation, *Cell 90*, 859−69.
53. Roux, P. P., Richards, S. A., and Blenis, J. (2003) Phosphorylation of p90 ribosomal S6 kinase (RSK) regulates extracellular signal-regulated kinase docking and RSK activity, *Mol. Cell. Biol. 23*, 4796−804.
54. Chebotareva, N. A., Kurganov, B. I., and Livanova, N. B. (2004) Biochemical effects of molecular crowding, *Biochemistry (Moscow) 69*, 1239−51.
55. Zhou, T., Sun, L., Humphreys, J., and Goldsmith, E. J. (2006) Docking interactions induce exposure of activation loop in the MAP kinase ERK2, *Structure 14*, 1011−9.
56. Liu, S., Sun, J. P., Zhou, B., and Zhang, Z. Y. (2006) Structural basis of docking interactions between ERK2 and MAP kinase phosphatase 3. *Proc. Natl. Acad. Sci. U.S.A. 103*, 5326−31.
57. Krishnaswamy, S., and Betz, A. (1997) Exosites determine macromolecular substrate recognition by prothrombinase, *Biochemistry 36*, 12080−6.
58. Bardwell, L., and Thorner, J. (1996) A conserved motif at the amino termini of MEKs might mediate high-affinity interaction with the cognate MAPKs, *Trends Biochem. Sci. 21*, 373−4.
59. Tanoue, T., Adachi, M., Moriguchi, T., and Nishida, E. (2000) A conserved docking motif in MAP kinases common to substrates, activators and regulators, *Nat. Cell Biol. 2*, 110−6.
60. Meng, W., Swenson, L. L., Fitzgibbon, M. J., Hayakawa, K., Ter Haar, E., Behrens, A. E., Fulghum, J. R., and Lippke, J. A. (2002) Structure of mitogen-activated protein kinase-activated protein (MAPKAP) kinase 2 suggests a bifunctional switch that couples kinase activation with nuclear export, *J. Biol. Chem. 277*, 37401−5.
61. Hill, J. M., Vaidyanathan, H., Ramos, J. W., Ginsberg, M. H., and Werner, M. H. (2002) Recognition of ERK MAP kinase by PEA-15 reveals a common docking site within the death domain and death effector domain, *EMBO J. 21*, 6494−504.
62. Brown, N. R., Noble, M. E., Endicott, J. A., and Johnson, L. N. (1999) The structural basis for specificity of substrate and recruitment peptides for cyclin-dependent kinases, *Nat. Cell Biol. 1*, 438−43.
63. Slupsky, C. M., Gentile, L. N., Donaldson, L. W., Mackereth, C. D., Seidel, J. J., Graves, B. J., and McIntosh, L. P. (1998) Structure of the Ets-1 pointed domain and mitogen-activated protein kinase phosphorylation site, *Proc. Natl. Acad. Sci. U.S.A. 95*, 12129−34.

BI0610451